X. Zhou[1], L. Duenas-Osorio[1], J. Doss-Gollin[1], L. Liu[2], L. Stadler[1, 3], and Q. Li[1, 3, 4, 5]

[1]Department of Civil and Environmental Engineering, Rice University, Houston, USA.

[2]Department of Civil, Construction and Environmental Engineering, Iowa State University, Ames, USA.

[3]Nanosystems Engineering Research Center for Nanotechnology-Enabled Water Treatment, Rice University, Houston, USA.

[4]Department of Chemical and Biomolecular Engineering, Rice University, Houston, USA

[5]Department of Materials Science and Nanoengineering, Rice University, Houston, USA

Corresponding author: Xiangnan Zhou (xz68@rice.edu)

Key Points:

- We develop a meso-scale representation model with reduced complexity for distributed water systems to enable computational policy search.
- We build a multi-objective optimization model to find the optimal allocation of direct potable reuse for economic and energy efficiency.
- Our case study reveals that location and available reuse capacity determine the benefits of distributed direct potable reuse.

Abstract

It is widely acknowledged that distributed water systems (DWSs), which integrate distributed water supply and treatment with existing centralized infrastructure, can mitigate challenges to water security from extreme events, climate change, and aged infrastructure. However, there is a knowledge gap in finding beneficial DWS configurations, i.e., where and at what scale to implement distributed water supply. We develop a meso-scale representation model that approximates DWSs with reduced backbone networks, which enable efficient system emulation while preserving key physical realism. Moreover, system emulation allows us to build a multi-objective optimization model for computational policy search that addresses energy utilization and economic impacts. We demonstrate our models on a hypothetical DWS with distributed direct potable reuse (DPR) based on the City of Houston's water and wastewater infrastructure. The backbone DWS with greater than 92% link and node reductions achieves satisfactory approximation of global flows and water pressures, to enable configuration optimization analysis. Results from the optimization model reveal case-specific as well as general opportunities, constraints, and their interactions for DPR allocation. Implementing DPR can be beneficial in areas with high energy intensities of water distribution, considerable local water demands,

and commensurate wastewater reuse capacities. The meso-scale modeling approach and the multi-objective optimization model developed in this study can serve as practical decision-support tools for stakeholders to search for alternative DWS options in urban settings.

Plain Language Summary

Distributed water systems that integrate localized water supply with existing centralized systems can improve the adaptability of urban water systems facing emerging challenges. Our study focuses on how to best allocate distributed direct potable reuse of municipal wastewater to supplement conventional water supply. We develop a system representation model that enables the policy search by representing a water system with reduced modeling complexity while retaining its key physical behaviors. We build a multi-objective optimization model upon it to find where and what scale to implement direct potable reuse to achieve system-wide energy and economic efficiency. We apply our models to design a hypothetical distributed water system based on the real water distribution and wastewater infrastructure data in the City of Houston, Texas. The reduced representation model shows large variations of energy intensity across the system, which informs the siting of distributed direct potable reuse. The policy search results show that distributed direct potable reuse can be competitive in areas where distribution energy intensities are high, and the direct potable reuse capacities are commensurate to local water demands. Methods developed in this study will serve as decision-support tools for urban water utilities to design distributed water systems that achieve system-wide goals.

1 Introduction

Urban water infrastructure systems face multiple acute and chronic stressors including increasing extreme events (e.g., floods), climate change (e.g., extended droughts), and aged infrastructure (Crosson et al., 2021; He et al., 2021; Flörke et al. 2018; Porse et al., 2018; Larsen et al., 2016; Gray, 2019; Diffenbaugh et al., 2015; Hering et al., 2013). Extreme events like floods can cause significant damage to water infrastructure systems leading to disasters (van de Lindt et al., 2020; Khan et al., 2015). Climate change threatens water quantity and quality available, as it can diminish groundwater recharge due to reduced precipitation and runoff (Alam et al., 2021; Gray, 2019). The majority of the water infrastructure in the U.S. was built 50 or more years ago, and these assets are now reaching the end of their design lives (AWWA, 2011; Leigh & Lee, 2019). Following decades of under-investment, the cost of maintaining existing levels of service may reach one trillion dollars, and the cost of adapting to stressors may be higher still (ASCE, 2021).

These challenges present an opportunity to rethink the 20^{th} century paradigm of highly centralized water systems (Larsen et al., 2016; Sharma et al., 2010). For example, distributed water systems (DWSs) that integrate water supply and treatment with existing centralized systems, such as direct potable reuse (DPR) located close to points of demand and resource availability, are a promising

emerging alternative (Liu et al., 2020; Zodrow et al., 2017; NRC, 2011; Sharma et al., 2010; Biggs et al., 2009). Figure 1 conceptually sketches a comparison between centralized water systems and DWSs. These DWSs are a subset of regional integrated water systems that manage various water infrastructure sectors (i.e., water distribution, wastewater, and stormwater). In this paper, we primarily focus on DWSs that integrate DPR, which reclaims potable water from municipal wastewater and directly distributes the reclaimed water to existing distribution infrastructure (Liu et al., 2020).

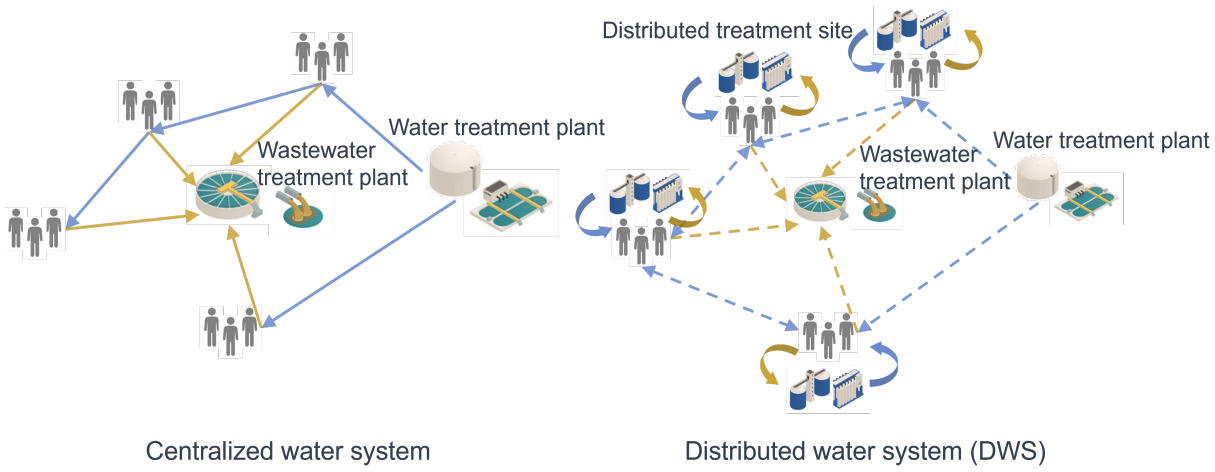

Figure 1. Conceptual comparison between centralized and distributed water systems. At each distributed treatment site, local wastewater collected is treated to potable standards and pumped to the existing water distribution system. The arrows indicate directions of water or wastewater flows. The solid lines represent that there are always water or wastewater flows, while the dashed lines denote that there may be water and wastewater flows. The dashed lines with double arrows indicate that water exchange among distributed treatment sites is flexible.

Previous work suggested that DWSs can improve robustness of water supply owing to their distributed topological structure (Zodrow et al., 2017; Hering et al., 2013; Makropoulos 2010; Biggs et al., 2009). In a DWS, local distributed supply forms subsystems linked with the centralized network for service supplement or back-up. In this way, the service loss from one subsystem or the centralized system can be compensated by increased production at others. Moreover, the distributed allocation enables flexible incremental investment and reconfiguration to adapt to local demographic (e.g., new customers), regulatory, or environmental conditions. In addition to benefits from robustness and flexibility, DWSs have the potential to reduce the environmental footprint of water supply and consumption. More localized supply takes advantage of local resources and reduces the energy needed to transport resources over long distances, possible waste (e.g., from leakage), and the load on physical components (Makropoulos

2010; Biggs et al., 2009).

Although these potential benefits suggest transitioning to DWSs that integrate substantial distributed components, there is limited knowledge about how to integrate distributed subsystems into existing centralized infrastructure. A particular challenge to overcoming this knowledge gap is modeling the hybrid centralized-distributed water systems at scales that are meaningful to answer policy questions. Policy search for DWSs usually requires system configuration optimization, the computational complexity of which is sensitive to the complexity of the system model. DWSs are complex socio-technical systems, and they can be characterized at multiple scales, from micro, to meso, to macro scales (Hoffmann et al., 2020; Diao, 2021). The system representation at multiple scales is concerned with system performance descriptions at individual end users scale (micro), community users (meso), and municipal or city users (macro). In a DWS, the integration of distributed subsystems occurs naturally at the meso scale, where the key modeling interest is the complex performance interaction between the distributed subsystems and the centralized system.

There are some recent studies on searching for alternative urban water systems based on system description at meso scales. Kavvada et al. (2018) developed a heuristic approach to estimate the financial cost, energy use, and greenhouse gas emissions associated with decentralized non-potable water reuse as a function of scale of treatment and conveyance networks, to determine community-scale optimal degree of decentralization. Jensen & Khalis (2020) developed a set of meso-scale performance indicators for local water systems to measure their water security levels and suggested their use to prioritize distributed water integration projects in areas with high water security risk, like Jakarta, Indonesia. Vitter et al. (2018) developed an optimal model for the sizing and hourly dispatch of a community-scale direct potable water recycling facility to minimize overall community costs under utility service balance constraints. Then, Jones & Leibowicz (2021) extended their work and developed a model to co-optimize community-scale distributed water reuse and energy operations. They found that co-optimized community-scale distributed electricity and water can achieve synergies that make it more attractive than the sum of household-level implementations by taking advantage of economies of scale, spreading out up-front costs over more households, and flexibly operating distributed water to consume surplus distributed electricity.

The existing quantitative meso-scale system models primarily focus on localized policy analysis, while do not account for the optimal coordination across the distributed subsystems and existing centralized systems. This paper develops a meso-scale representation model based on a flow hierarchy characterization technique to approximate large water systems by their meso-scale backbone networks, which allows for a computationally efficient representation while maintaining key physical behaviors. As a result, this meso-scale representation facilitates the application of policy search algorithms to the generation of alternative system configurations. We apply this method to a hypothetical DWS based

on the City of Houston's existing water and wastewater infrastructure. The meso-scale DWS representation enables a multi-objective optimization analysis to identify which existing wastewater treatment plants (WWTPS) to implement DPR on, and what the appropriate treatment scales are, to optimize the overall system's financial cost and energy consumption. The meso-scale modeling method and the associated multi-objective optimization model developed in this study show how to plan and design DWSs that exploit the performance interplay between distributed subsystems and the global system.

We organize the rest of this paper as follows. Section 2 introduces the fundamental methods for our meso-scale system modeling and policy search. Then, section 3 demonstrates a practical case application of our modeling approaches and shows case-specific insights about modeling and system design. Finally, section 4 concludes this study with key highlights, limitations, and future research directions.

2 Methods

Our modeling framework includes two parts: the meso-scale modeling and the policy search, as illustrated by Figure 2. The meso-scale model includes three sub models: (1) the water network model, which represents a water distribution system with a hydraulic-informed complex network; (2) the hierarchical characterization model, which reveals the multi-scale structure of a water network through complex network analysis and identifies critical components, high in the hierarchy; and (3) the backbone network extraction model, which builds a reduced network that contains components of high hierarchy levels, while approximating the hydraulic boundary conditions of the complete network through an aggregation algorithm. The backbone network yields a reduced representation featuring key physical behaviors at the interface between the global and local subsystems. In addition, this backbone makes many-query policy search across design options tractable. The backbone is then fed to the multi-objective optimization model to search for ideal locations and treatment scales of distributed DPR to optimize system-wide energy consumption and economic cost.

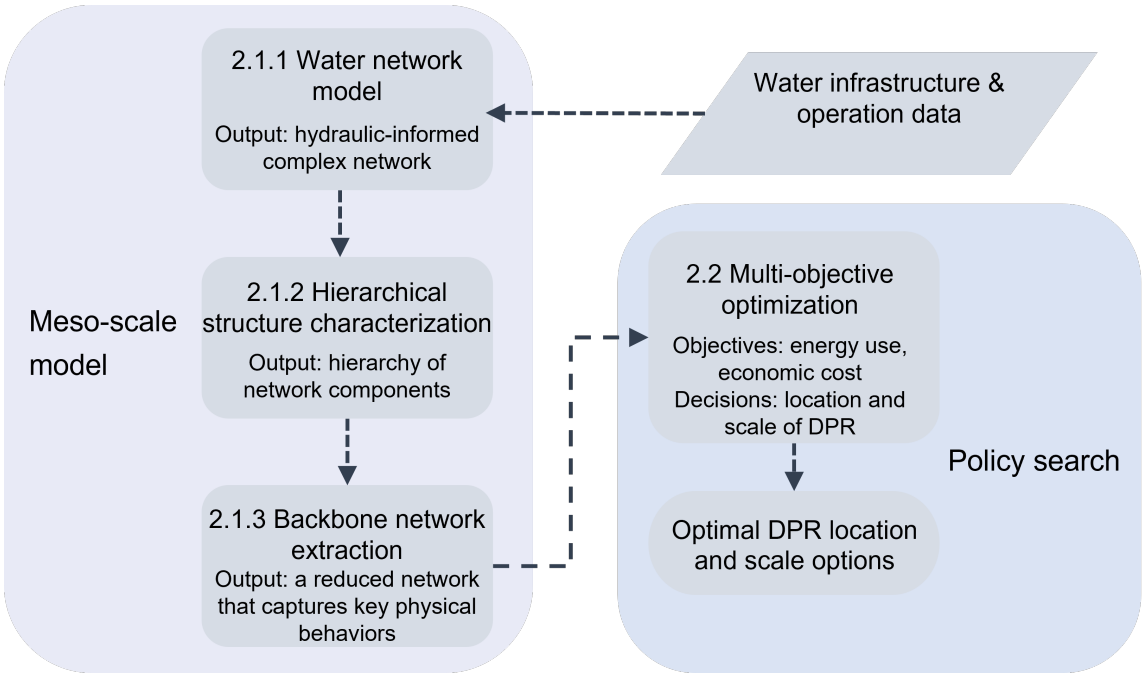

Figure 2. Schematic of our modeling framework.

2.1. Meso-scale model

2.1.1. Water network model

The primary service of a water distribution system is to deliver water of adequate quantity, pressure, and quality to consumers. We model a water distribution system with a directed network $G = (N, E)$, where N is the set of nodes representing water treatment plants (WTPs), storage tanks, demand nodes, and non-demand pipe junctions, and E is the set of directed edges denoting pipes, pumps, and valves. A directed edge $e_{i,j}$ is established if there is water flow from node i to its adjacent node j. Each node i has its node properties such as node demand D_i, and each edge $e_{i,j}$ possesses edge properties like water flow $Q_{i,j}$.

There are two basic governing equations for a water distribution network G: the mass balance equation at each node i [Equation (1)], and the energy conservation equation along each edge $e_{i,j}$ [Equation (2)]. The mass balance equation governs the water quantity allocation within G:

$$\sum_{m \in N_{\text{in}}(i)} Q_{m,i} - \sum_{j \in N_{\text{out}}(i)} Q_{i,j} = D_i \quad (1)$$

where $N_{\text{in}}(i)$ and $N_{\text{out}}(i)$ denote the set of nodes from which incoming flows to node i come and the set of nodes to which outgoing flows from node i go,

respectively, D_i is the demand value of node i. The energy conservation equation relates the water flow quantity and water head change along edges. As for an edge $e_{i,j}$ that represents a dissipation element like a pipe or a valve, the water head H_i at the start node i is always greater than that at the end node j with a positive $h_{i,j}$. If an edge $e_{i,j}$ corresponds to an element with energy-injection like a pump, $h_{i,j}$ is negative representing a head gain.

$$H_i - H_j = h_{i,j} \quad (2)$$

The head loss $h_{i,j}$ is determined by $Q_{i,j}$ and the energy needed to overcome gravity and friction, while the head gain $h_{i,j}$ is determined by $Q_{i,j}$ and the energy provided to uplift the flow.

For the computational implementation, we use a Python package WNTR (Klise et al., 2017), which is based on hydraulic and water quality analysis algorithms of the widely used EPANET software (EPA, 2020). We use it to perform steady-state hydraulic simulations that produce hydraulic attributes essential for establishing hydraulic-informed complex networks, illustrated as step 2.1.1 in Figure 2.

2.1.2. Hierarchical structure characterization

The hierarchical structure in a complex network emerges from the different roles of the nodes or edges (Pumain, 2005; Gómez et al., 2013; Ferrario et al., 2016). A directed water network G that represents a water distribution system usually has a flow hierarchy, where water flows from sources (i.e., WTPs) through distribution mains to local storage tanks and then to downstream consumer connections. Nodes N can be layered in different hierarchical levels so that the incoming and outgoing flows of nodes at upper levels determine the incoming and outgoing flows of nodes at lower levels.

Our goal of hierarchical structure characterization is to identify a set of critical nodes that retain the critical topological features and hydraulic behaviors of a water network G. These nodes will be candidates for a backbone network that approximates G with reduced complexity. In a directed water network G, we define the criticality level of a node i as the degree to which it contributes to routing the water flows. We introduce a metric named local reaching centrality $C_R(i)$ developed by Mones et al. (2012) to quantify the criticality level of a node i in G. The metric is developed to characterize the flow hierarchy in a network, which is a key feature of large water systems. For an unweighted directed network, $C_R(i)$ quantifies the proportion of all nodes in the graph that can be reached from node i via outgoing edges. In a weighted directed network, $C_R(i)$ is defined as:

$$C_R(i) = \frac{1}{n_N - 1} \sum_{j:\ 0<d^{\text{out}}(i,m)<\infty} \frac{\sum_{k=1}^{d^{\text{out}}(i,m)} w_{i,m}^{(k)}}{d^{\text{out}}(i,m)} \quad (3)$$

where n_N is the total number of nodes, $d^{\text{out}}(i,m)$ is the length of the shortest directed path that goes from i to m via out-going edges, and $w_{i,m}^{(k)}$ is the weight of the k^{th} edge along this path. Link weight is assumed to be proportional to the connection strength. As for a water distribution network G, we interpret the connection strength of an edge $e_{i,j}$ as its capability to route water flows. We define the hydraulic-informed weight $w_{i,m}^{(k)}$ of the k^{th} edge as the product of its water flow rate $Q_{i,m}^{(k)}$ and its cross-section area $A_{i,m}^{(k)}$. The former represents the current flow rate determined by both its flow velocity and its cross-section area, while the latter considers its potential flow capacity in the future for a given range of flow velocities. If node i and j are connected by more than one directed shortest path, then the one with the maximum weight is used.

We calculate the local reaching centrality $C_R(i)$ of each node i following Equation (3) and rank them accordingly. Clusters of nodes of high hierarchy levels can be identified from the distribution of $C_R(i)$. Sometimes, distinct gaps exist in the distribution plot for $C_R(i)$, indicating the presence of definite hierarchy layers. In this case, we can select critical nodes considering the representation level of interest and the hierarchy clustering pattern. Otherwise, we need to select critical nodes by specifying a practical threshold (e.g., 80^{th} percentile of the local reaching centrality values) determined from the reduction level of interest.

2.1.3. Backbone network extraction

A backbone water network G_B is a subnetwork that preserves the critical topological and hydraulic behaviors of the complete water distribution network G with reduced size and complexity. The concept of backbone extraction has been studied in the fields of physics (Gemmetto et al., 2017), sociology (Neal, 2014), biology (Darabos et al., 2014), computer science (Foti et al., 2011), and infrastructure networks (Dai et al., 2018; Ducruet, 2017). In the field of infrastructure networks, backbone extraction for transportation networks receives great interest in tracing dynamics and uncovering their underlying mechanisms (Dai et al., 2018).

Generally, backbone extraction techniques for infrastructure networks are edge-removing techniques that focus on finding the most critical nodes and edges and subsequently eliminating the least significant ones (Dai et al., 2018). Different backbone extraction techniques use different criteria for identifying node/edge importance to the network. As for a water distribution network G, the most relevant features are the hydraulic attributes at service nodes. Therefore, we adopt a node-dominated backbone extraction approach and build the backbone network from nodes of functional criticality.

The nodes of functional criticality are identified from the hierarchical struc-

ture characterization of the hydraulic-informed network. Given critical nodes to preserve for the network approximation, we build a backbone network G_B following two steps: (1) find the largest network component G_C that connects critical nodes with all the sources through hydraulic-informed shortest paths; (2) establish hydraulic boundary conditions for G_C by aggregating demands of all the removed nodes to their upstream, retained nodes.

Our aggregation algorithm builds upon the flow backtracking algorithm in Liu & Mauter (2021), which backtracks water delivered to each consumer to its sources and the energy consumption along the flow paths, and the onion decomposition algorithm (Hébert-Dufresne et al., 2016). The core part of the backtracking algorithm is to calculate the fraction of water received by consumer j that comes from injection point i at time t, $r_{i,j}(t)$, assuming each node in the water network is a perfect mixer of the upstream water it receives. As illustrated by Equations (4) and (5), $r_{i,j}(t)$ is calculated recursively from $r_{i,u}(t)$, where U is the set of the immediate upstream nodes of j, and $Q_{u,j}(t)$ is the water flow rate from node u to node j.

$$r_{i,j}(t) = \sum_{u \in U} r_{i,u}(t) r_{u,j}(t) \quad (4)$$

$$r_{u,j}(t) = \frac{Q_{u,j}(t)}{\sum_{u \in U} Q_{u,j}(t)} \quad (5)$$

The flow backtracking algorithm is a disaggregation algorithm that starts from the sources and disaggregates flow and energy to downstream nodes recursively. Our aggregation algorithm goes instead from downstream to upstream leveraging Equation (5) and the onion decomposition algorithm to aggregate demands of downstream nodes to their nearest upstream nodes in backbone network G_B. The onion decomposition algorithm prioritizes removal of nodes from a network according to their connectivity degrees. The reader can refer to Text S1 in the Supporting Information for a detailed description of the aggregation algorithm.

Note that although the concept of skeletonization is relevant, it is different from our backbone representation. Skeletonization, which usually includes branch trimming, node aggregation, merging of series or parallel pipes, and removal of nonessential components (Walski et al., 2003), has been widely used to simplify the modeling of a water distribution system for practical application. The primary difference between backbone extraction and skeletonization is that the former is based on global behavior characterization while the latter depends on local equivalence. Skeletonization can only achieve a limited degree of reduction due to its underlying logic of local approximation, while the backbone extraction is more compressed while preserving a multi-scale critical structure.

2.2. Multi-objective optimization

There are multiple critical criteria such as economic cost, energy usage, environmental footprint, and system resilience to consider when exploring alternative water management strategies (Englehardt et al., 2016; Crosson et al., 2021).

Our multi-objective optimization model addresses a subset of these metrics, the economic cost and energy usage, which are immediate to utilities. The system-wide economic cost and energy use of a DWS with distributed DPR depend on the DPR technology, the scale of DPR plants (Sim & Mauter, 2021), and their integration locations. These factors determine local- and global-level economic costs and energy consumption as well as their interactions.

At the local level, the financial investment and energy consumption increase with the scale of a DPR facility with specific economies of scale depending on the treatment technology adopted. Advanced water treatment facilities are needed to treat reclaimed water to potable standards, which is usually of superior quality. The current advanced treatment facilities tend to be more energy and cost expensive than the conventional surface WTPs (Englehardt et al., 2016; Sim & Mauter, 2021).

At the global level, distributed DPR reduces the energy required for conveyance, especially for those service areas far from the surface WTPs. Also, distributed water supply can reduce economic investment needed for upgrading or expanding centralized infrastructure. In addition, implementing distributed DPR reduces freshwater withdrawal or import, and discharge of wastewater into natural aquatic environment yielding system-wide economic and environmental benefits.

We formulate a multi-objective optimization model to exploit the complex interaction between the performance of local DPR plants and the overall system-wide performance of the DWS. Performance objectives include economic cost and energy consumption related to infrastructure investment, water treatment, and water distribution. The benefits relevant to improved water quality, improved system supply resilience, reduced freshwater withdrawal and wastewater discharge are not reflected in our cost analysis yet due to limited study on their estimation. The decision variables are locations and treatment scales of DPR facilities. The constraints are local and global demand satisfaction, the available sites for DPR plants, which are assumed to be on the sites of existing WWTPs, the capacities of DPR plants, which are determined by capacities of their corresponding WWTPs, as well as hydraulic and operational requirements.

We model the DPR allocation within a reduced backbone network G_B as a multi-objective nonlinear programming problem with two objectives and five constraints. The objectives are minimizing the total economic cost, f_1 in Equation (6), and energy consumption, f_2 in Equation (7). We formulate the problem as follows:

$$\min(f_1) = \sum_c C_c(S_c) + \sum_c O_c(S_c) + \sum_p C_p(S_p) + \sum_p O_p(O_p) \quad (6)$$

$$\min(f_2) = \sum_c e_c S_c + \sum_p e_p S_p + g(S_c,\ S_p) \quad (7)$$

Subject to:

Equation (1), (2)

$$S = \sum_c S_c + \sum_p S_p \quad (8)$$

$$S_p \leq U_p \quad (9)$$

$$c \in \{\text{conventional WTPs}\},\ p \in \{\text{DPR plants}\}$$

where S_c and S_p are the supply amounts at conventional WTPs and DPR plants, respectively. Regarding f_1, we denote $C_c(S_c)$ as the capital cost to build new or to expand conventional WTPs and other water supply infrastructure, and $O_c(S_c)$ as the operation and maintenance (O&M) cost to run the infrastructure. The capital investment usually includes costs for land use, treatment equipment, and infrastructure (e.g., pipes and pump stations), while the O&M cost covers electricity, chemicals, materials, and labor. Terms $C_p(S_p)$ and $O_p(S_p)$ represent the capital cost to establish DPR plants and the O&M cost to run them, respectively. As for f_2, we have e_c and e_p as energy intensities of conventional and DPR treatment, respectively. The term $g(S_c,\ S_p)$ is the energy function for distribution for a given DPR allocation configuration–usually a nonlinear function of supply amount S_c and S_p reflecting local-global interaction of water distribution.

Constraints in Equations (1) and (2) are hydraulic laws for mass balance and energy conservation within the backbone network G_B of the DWS. Equation (8) ensures that water supply from all plants meets the total system demand S, guaranteeing customer satisfaction. Equation (9) is the capacity constraint indicating the maximum DPR supply U_p available at each DPR site considering the reclaim rate and the capacity of its corresponding WWTP.

As for multi-objective optimization problems without a prior preference information (e.g., weights of the objectives), we cannot directly compare the values of one objective function with those of another objective function. An effective way to deal with this situation is to use *dominance* to determine the goodness of a solution. Solution 1 dominates solution 2 if solution 1 is no worse than solution 2 in all objectives, and solution 1 is strictly better than solution 2 in at least one objective. Then, the ultimate goal of solving a multi-objective optimization problem becomes finding the non-dominated solution set, also called the Pareto-optimal set, where none of the objectives can be improved without deteriorating one of the others. Because analytical solutions to this nonlinear problem are not available, we use a widely applied heuristic algorithm, the Non-dominated Sorting Genetic Algorithm-II (Deb et al., 2002), to solve this multi-objective optimization problem. We validate computation by examining an empirical convergence indicator, the hypervolume, over the solving proce-

dure. The principal workflow of the solving algorithm is demonstrated in Text S2 in the Supporting Information.

3 Case study and results

3.1. City of Houston application

We demonstrate the meso-scale modeling approach and the multi-objective optimization model developed in this paper on a hypothetical yet realistic DWS. The system includes the real water distribution system of the City of Houston (denoted as Houston in the following), Texas, and hypothetical DPR sites located at 15 of the existing 39 WWTPs in Houston. It will be referred as Houston DWS in the following. We selected 15 WWTPs because they have publicly available influent flow data. Their capacities are greater than 1.6 million gallons per day (MGD) ($6.056 \times 10^6 m^3/d$). Houston's water distribution system is complex (see Figure 3) with thousands of interconnected components, serving an average of 460 MGD ($2.091 \times 10^6 m^3/d$) of water through approximately 7000 miles (1.126×10^4km) of pipes [Houston Public Works, 2021 (a)]. Houston operates three surface WTPs, the East, Southeast, and Northeast Water Purification Plants, all of which are located on the east side of the city. The current capacities of the East, Southeast, and Northeast Water Purification Plants are 300 MGD ($1.364 \times 10^6 m^3/d$), 200 MGD ($9.092 \times 10^5 m^3/d$), and 65 MGD ($2.955 \times 10^5 m^3/d$), respectively [Houston Public Works, 2021 (b)]. The surface water comes from lakes and reservoirs in northeast Houston, which provides around 88% of its 460 MGD daily demand, with the East, Southeast, and Northeast Water Purification Plants providing an average of 243 MGD ($9.215 \times 10^5 m^3/d$), 116 MGD ($4.393 \times 10^5 m^3/d$), and 48 MGD ($1.820 \times 10^5 m^3/d$), respectively. The rest of the water supply is provided by groundwater treatment plants (GWTPs), most of which are located on the west side of the city. The system's 24-hour demand profile is shown in Figure S2 in the Supporting Information. The green stars in Figure 3 represent the 15 large WWTPs in Houston that we use as potential DPR sites.

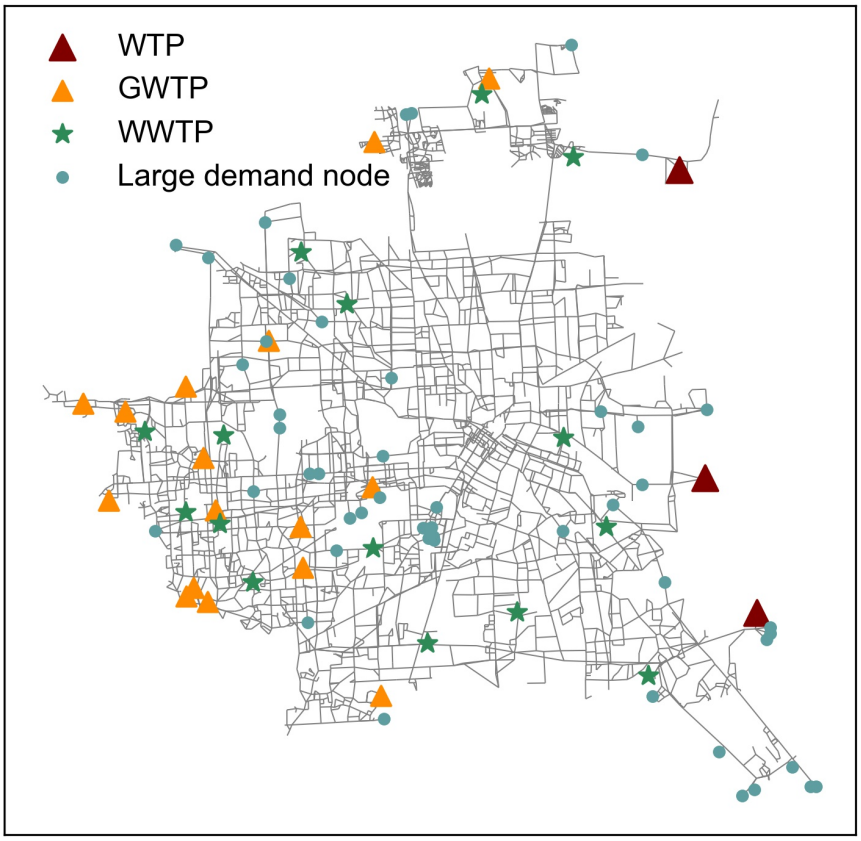

Figure 3. Schematic representation of Houston's water distribution system and 15 WWTPs for DPR. Gray lines indicate the distribution pipes, pumps, and valves. A large demand node refers to a node whose daily demand is equal to or greater than the 99^{th} percentile of demands of all nodes ($2.259 \times 10^3 m^3/d$).

Houston is an interesting testbed to explore integrating distributed DPR with existing water infrastructure to supplement conventional surface water and groundwater supply. In particular, there is a geographic mismatch between surface water supply and growth in municipal water demand as the largest portion of the population and the fastest population growth are on its west side opposite to locations of WTPs (Liu et al., 2020). Additionally, Houston experiences land subsidence and seawater intrusion due to groundwater withdrawal (Herrera-García et al., 2021; Jasechko et al., 2020). The Harris-Galveston Subsidence District expects to reduce reliance on groundwater to mitigate ground subsidence (Harris Galveston Subsidence District, 2019). Moreover, Houston is a flatland with slight elevation variation, thus, a large amount of treated water needs to be pumped miles westward from the WTPs on the east. The long-distance water conveyance poses a significant load burden on the water

infrastructure and increases the system's vulnerability to disruptions.

3.2. The meso-scale backbone network

We implement our modeling framework illustrated by Figure 1 on Houston DWS to obtain its meso-scale representation as follows. First, we perform steady-state hydraulic simulation at hourly resolution and build the hydraulic-informed water network G^* that represents the water flows at a peak hour, 7:00 a.m. (see Text S3 in the Supporting Information for the reason to adopt the peak-hour as the representative state). Second, we evaluate the local reaching centrality $C_R(i)$ for each node i in G^* using Equation (3) in section 2.1.2 and identify critical nodes at high hierarchy levels. The distribution of normalized $C_R(i)$ is shown in Figure S3, while the critical nodes identified are shown in Figure S4, both in the Supporting Information. Then, applying the backbone extraction approach described in 2.1.3, we extract the backbone water network G_B^*, as shown by Figure 4. The backbone water network G_B^* preserves 290 edges, a 95% reduction from the existing network, and 269 nodes, a 93% reduction. Note that optimization analysis of complex networks is usually combinatorial such that the computational complexity scales at least the polynomial of the network size. The backbone network makes computational policy search feasible by greatly reducing the computational load of optimization analysis.

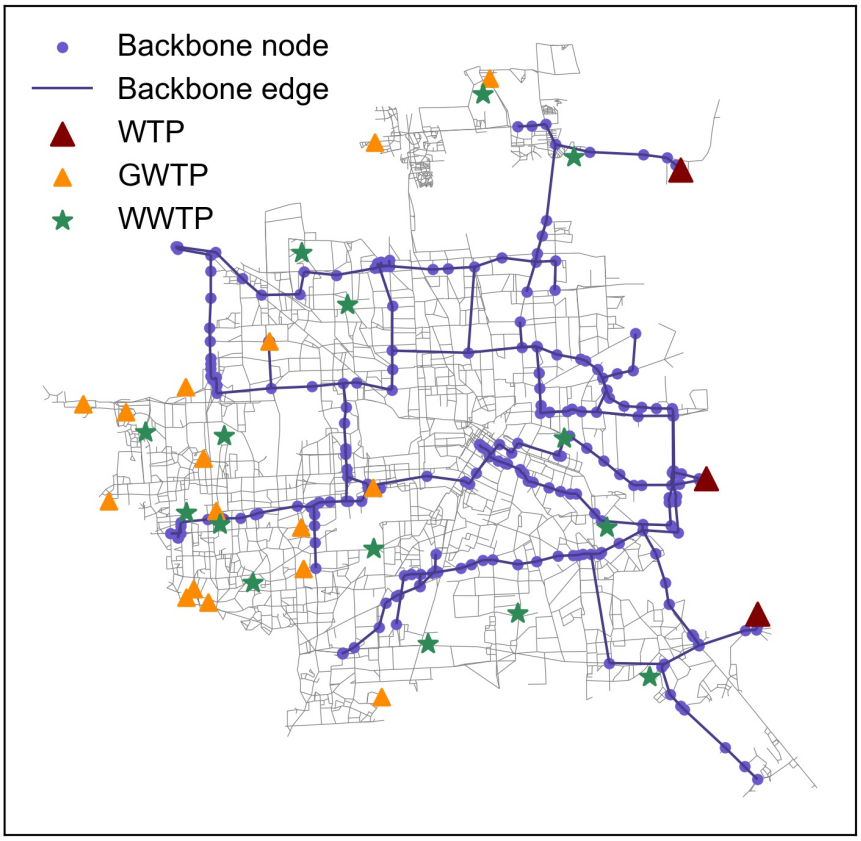

Figure 4. The meso-scale backbone network with 290 edges (95% reduction) and 269 nodes (93% reduction) laying over the existing water distribution system.

To demonstrate that the backbone water network G_B^* preserves key macro- and meso-scale behaviors of the full water network G^*, we compare their basic hydraulic measures, water flows, and pressures. We keep all the operational settings of the remaining pumps and valves in the backbone network the same as those of the full network. As for the water flows, we examine macro flow measures in G^* and G_B^*, i.e., outflows from WTPs, as shown in Table 1. The outflows at WTPs vary along with changes of hydraulic boundary conditions. We achieve a relatively good approximation of water flows at the macro scale with the total relative difference being -1.44%.

Table 1. Outflow values at the surface WTPs $[m^3/s]$.

WTPs	Outflow (G^*)	Outflow (G_B^*)	Relative difference
East Water Purification Plant	11.121	11.402	1.12%
Southeast Water Purification Plant	5.372	4.804	-9.56%

Northeast Water Purification Plant	2.140	2.158	0.75%
Total	18.633	18.364	−1.44%

Regarding pressures, Figure 5 (a) shows their distribution for the backbone water network G_B^*, while Figure 5 (b) gives the relative differences between G_B^* and G^*. The distribution of the relative difference is given in Figure S5 in the Supporting Information. The relative difference at the majority (81%) of nodes is within the range [−10%, 10%]. We also examine the daily pressure variations in G^*, the maximum relative difference to the mean pressure, 67% of the nodes have daily pressure variations within the range [−10%, 10%], as given in Figure S6 in the Supporting Information. The relative difference is within the reasonable variation bounds for regular operation.

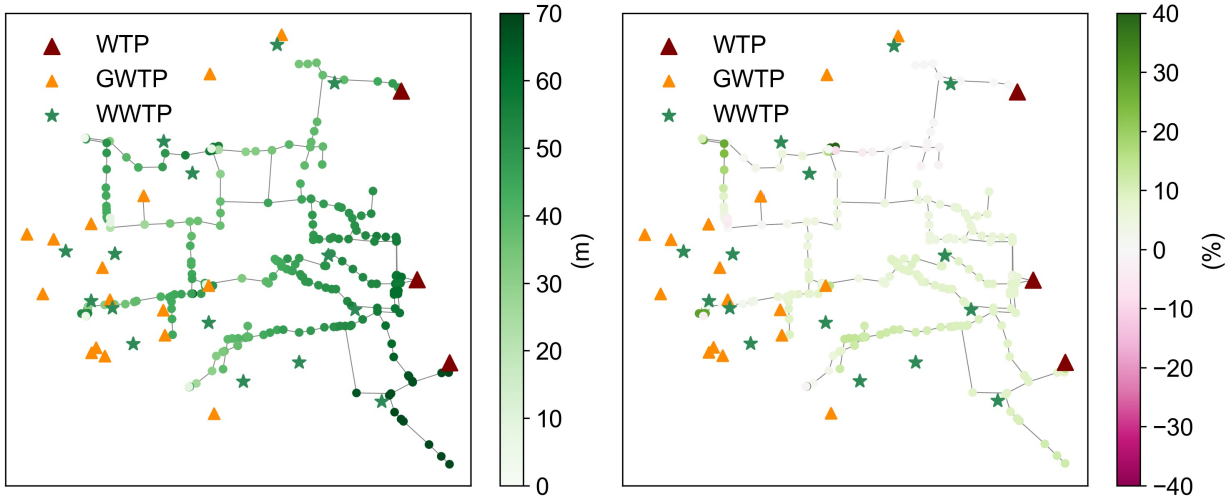

1. **(b)**

Figure 5. (a) Node pressure in the backbone water network G_B^*. **(b)** Relative difference of node pressures in G_B^* to those in the full water network G^*.

In addition, with the meso-scale backbone network G_B^*, we are able to examine performance measures that are critical for DWS configuration design but not tractable with the full water network G^*. Figure 6 (a) shows the meso-scale spatial distribution of water demands in G_B^*. The full water network G^* with redundant intricacy and a large number of connections clouds the spatial distribution of water demands in the system (see Figure S7). In addition, Figure 6 (b) shows the marginal energy intensities for distribution as in Liu & Mauter (2021). We see energy intensity increasing from the east to the west side of the system. This energy intensity estimation, which informs DWS configuration design, is also only tractable with the reduced backbone network G_B^*.

Also, our meso-scale performance characterization enables preliminary system design of DWSs. Considering the spatial distribution of water demands and marginal energy intensities obtained, we further narrow down to 10 of the 15 WWTPs (as indicated in Figure 6) as alternative DPR plants that can provide potential benefits through replacing local groundwater or surface water supply. The 5 WWTPs we drop are ones that cannot beat the surface WTPs in terms of energy efficiency in the near future. They are located in areas where the distribution energy intensities are lower than $0.4kWh/m^3$, while the current treatment energy intensities for DPR are likely to be higher than this level (Sim & Mauter, 2021).

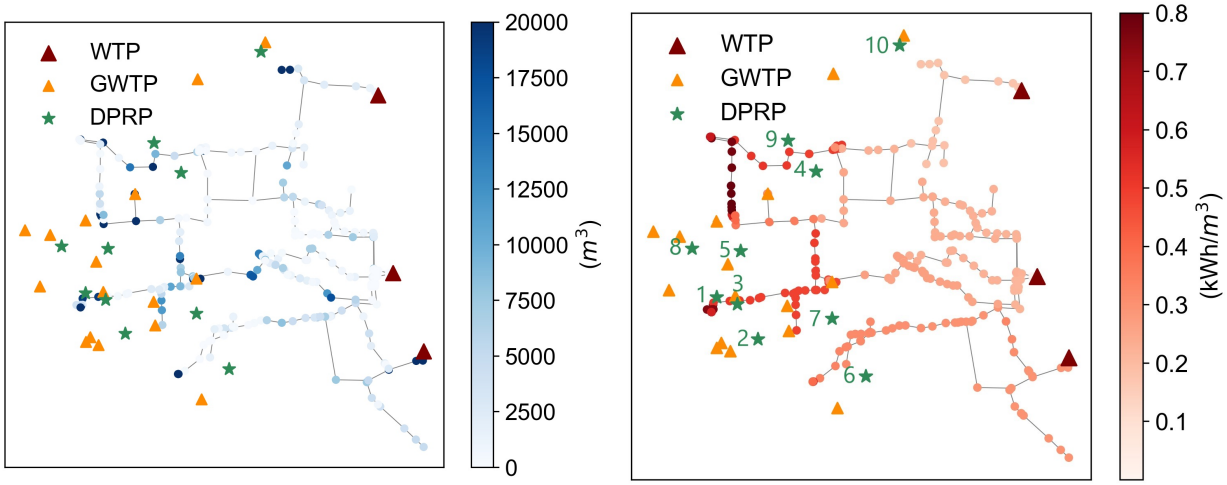

1. **(b)**

Figure 6. **(a)** Daily node demand in the backbone water network G_B^*. There is a significant variation of node demands, hence, the range of the colormap is less than the demand range, with the nodes of the darkest color all having demands larger than 20000 m^3. **(b)** Energy intensities for distribution in the backbone water network G_B^*.

Our final meso-scale Houston DWS model includes the backbone water network G_B^* , 10 alternative DPR plants, and 15 GWTPs. Each DPR plant has an upper bound of daily capacity determined by the daily flow capacity of its corresponding WWTP and its reclamation rate, which is assumed to be 80% (Liu et al., 2020). The backbone water network G_B^* takes hourly water allocation, and we assume that the daily DPR capacity is allocated following the same hourly demand pattern of the water distribution system. We use this proportional approximation scheme to calculate the energy and the economic impacts of Houston DWS. We model the distributed DPR plants by adding extra source elements that can replace the groundwater supply nearby it or supplement the demands of their nearest nodes in the backbone water network. The nearby threshold is set as $3000m$ considering the empirical service coverage area of the

GWTPs.

3.3. Pareto-optimal DPR allocation configurations

We implement our multi-objective optimization model on the meso-scale Houston DWS model to find Pareto-optimal DPR allocation configurations. We consider the status quo development scenario, in which there is no increased water demand to be met by extra infrastructure, and the DPR replaces part of existing groundwater or surface water supply. To evaluate Houston DWS's energy and economic impacts, we feed practical data (see Table 2) into Equations (6) and (7). The constraints with respect to DPR capacity and water supply balance are always guaranteed by specifying a satisfying search space. The hydraulic consistency constraints are satisfied by integrating hydraulic simulation with the NSGA-II solver. We use the python package Pymoo (Blank & Deb, 2020) to solve our optimization problem with its embedded NSGA-II solver. An empirical performance indicator, hypervolume, is used to examine the convergence of the solving procedure (see Text S4 in the Supporting Information).

Table 2. Key input data for the multi-objective optimization analysis.

Data	Value
Energy intensity of groundwater withdrawal	1.0 kWh/m^3
Energy intensity of surface water treatment	0.11 kWh/m^3
Energy intensity of advanced treatment for DPR	0.8, 0.4 kWh/m^3
Annual O&M cost rate of surface water treatment plant	\$ 167.30 $m^{-3}d^{-1}$
Annual O&M cost rate of DPR plant, $y = Ax^b$, unit of y : $\$m^{-3}d^{-1}$, unit of capacity x : m^3d^{-1}	$A = 386.9,\ b = -0.095$
Capital cost rate of DPR plant (25-year lifetime), $y = Ax^b$, unit of y : $\$m^{-3}d^{-1}$, unit of capacity x : m^3d^{-1}	$A = 18740,\ b = -0.21$

Regarding energy impacts, we use the energy intensities of surface water treatment and groundwater withdrawal in Liu et al. (2020), which are derived from the city's actual operation data and other field estimates (Twomey & Webber, 2011; Zhang et al., 2016). Energy intensities for advanced treatment processes vary greatly. Sim & Mauter (2021) aggregated a total of 70 operating, demonstration, pilot, and unbuilt potable water reuse systems in the U.S. and reported the cost and energy intensity reference for advanced treatment processes. The full range of energy intensity for advanced treatment is $[0.23,\ 2.5\ kWh/m^3]$,

while the 25^{th} and the 75^{th} percentiles of the energy intensities of advanced treatment taking secondary effluent are 0.8 kWh/m^3 and 1.8 kWh/m^3, respectively. We take two representative energy intensities for DPR: 0.8 kWh/m^3 and 0.4 kWh/m^3, which are assumed to be the energy intensity of advanced treatment, which treats secondary effluents discharged from the WWTPs to DPR standards. For the current Houston DWS, if the energy intensity of DPR is higher than 0.8 kWh/m^3, its potential benefits of energy efficiency will be limited. These choices represent optimistic expectations about the energy impact of advanced treatment technologies.

As for the economic cost estimation, implementing DPR introduces extra economic investment in the status quo planning setting. We only consider the annual O&M costs for the conventional WTPs and GWTPs, which are estimated from the utility's historical operational data (Houston Public Works, 2019). We adopt the regressed normalized cost curves developed by Sim & Mauter (2021) to estimate the annual capital and O&M costs for DPR. The capital cost does not include that of the extra distribution infrastructure (e.g., pipes and pump stations), which accounts for less than 2% of total capital cost according to Liu et al. (2020). The total capital cost is amortized to annual loan payments (see Text S5 in the Supporting Information).

Figure 7 shows the Pareto fronts obtained for two parameter settings revealing the trade-offs between economic cost and energy consumption. Our Pareto front has turning points corresponding to the launch of a new DPR plant, while each slightly curved line between turning points shows some nonlinear economic and energy impacts. The upper right Pareto fronts consists of almost vertical lines with vertically jumping solution points, indicating that adding DPR cannot provide any more energy benefits.

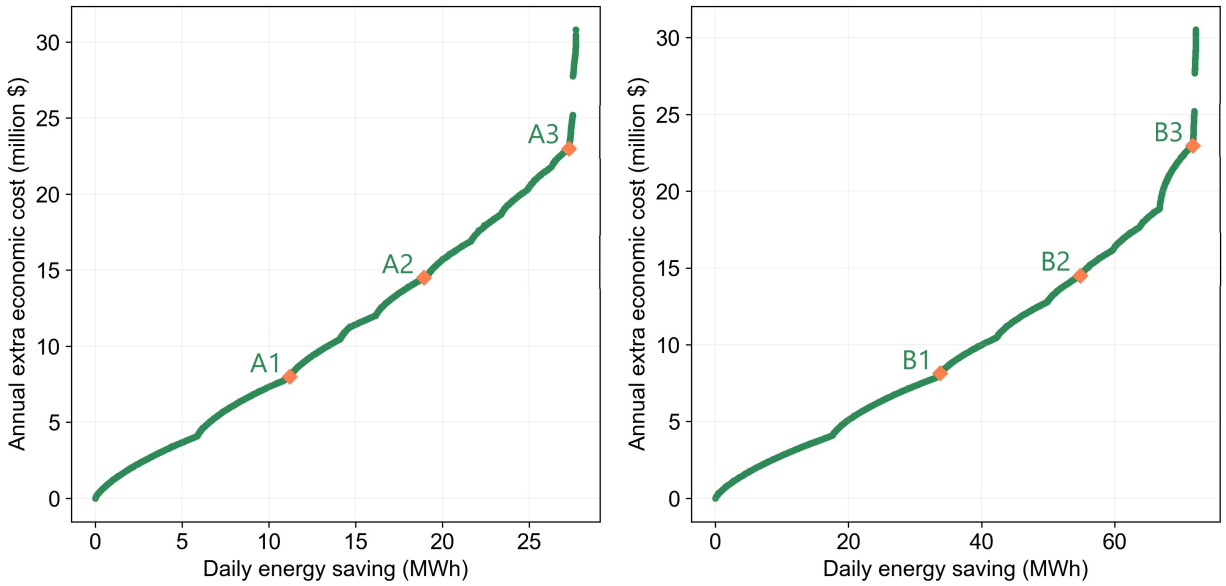

(a) $e_d = 0.8$ kW$h \cdot m^{-3}$ **(b)** $e_d = 0.4$ kW$h \cdot m^{-3}$

Figure 7. Pareto fronts for the annual extra economic cost and daily energy savings between Houston DWS and the existing system. Each part is for a specific energy intensity of DPR treatment, e_d.

We zoom into three representative configurations (see Figure 8), which are turning points of the Pareto fronts. Configuration A1, A2, and A3 have the same y-axis values with configuration B1, B2, and B3, respectively. Configuration A1 identifies plants 2 and 5 for DPR implementation to replace groundwater supply (same identification for B1—not shown). Plants 2 and 5 are located in areas requiring a great amount of groundwater supply, which is more energy intensive than DPR. Configuration A3 is a critical bound, beyond which adding DPR allocation is not beneficial anymore as the economic cost soars vertically. Configuration B3 makes very similar choices to A3 (not shown). They represent the "upper bound" of beneficial DPR integration for the current spatial distributions of energy intensities, water demands, and DPR capacities.

Configuration A2 has a different DPR allocation arrangement relative to configuration B2, as shown in Figures 8 (c), (d). However, if given the same DPR energy intensity, their daily energy savings are the same. The difference comes from performing global searches over the decision space, particularly when different decision variables share the same objective function values. While both configurations open plant 8 to replace groundwater compared to A1 (B1), configuration A2 chooses plant 4 to supplement surface water supply, while B2 launches plant 6 and 7 to replace groundwater. The two small plants 6 and 7 together have similar economic impact with that of the larger plant 4 due to the economies of scale. However, energy benefits of these small plants are

higher as they replace groundwater supply. The DPR volume of configuration A2 and B2 account for 7.0% and 6.4% of total supply, respectively. If we consider a third dimension, freshwater withdrawal, we will pick configuration A2 over configuration B2.

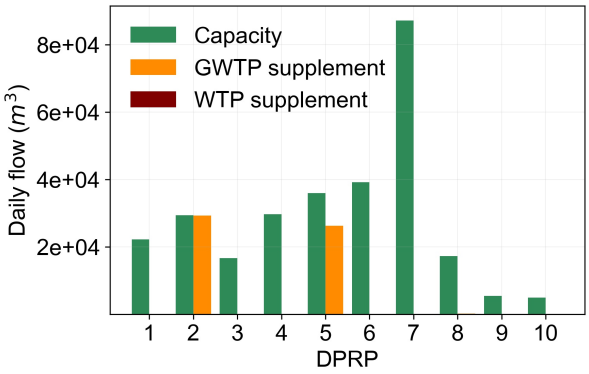

(a) Configuration A1

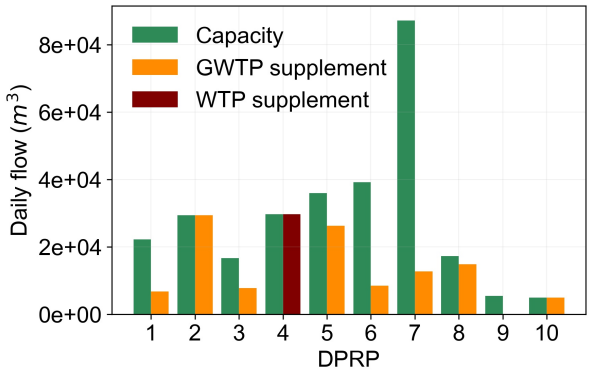

(b) Configuration A3

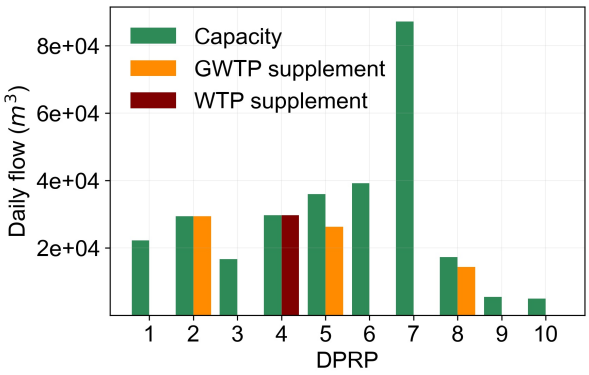

(c) Configuration A2

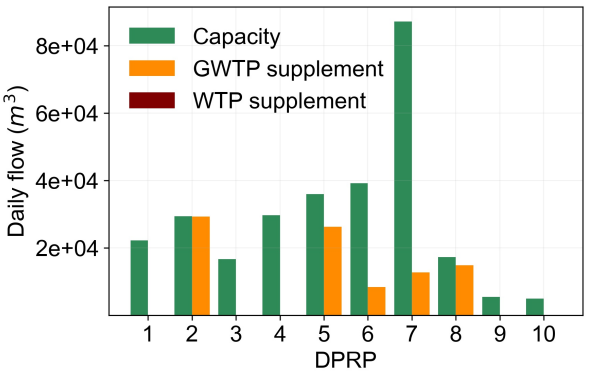

(d) Configuration B2

Figure 8. DPR allocation configurations for representative configurations in Figure 7.

Overall, the priority to implement DPR at potential plants depends on the location of the plant as well as its capacity given the complex local-global performance interaction. Location determines whether there is an opportunity (or not) to supplement groundwater or surface water of high distribution energy intensities to achieve energy savings. In our testbed, with no available DPR plant near the northwest of the system, the highest energy intensities for distribution remain an issue. As for the capacity of a plant, it determines whether it is economically efficient to implement DRP given a certain economic impact function. The appropriate places to implement DPR are western areas where the energy intensities of conventional supply are high, the water demands are considerable

and locally concentrated, and there are wastewater reuse capacities that match the magnitudes of water demands. The multi-objective optimization via the backbone network together unravels practical case-specific as well as general opportunities, constraints, and their interactions for DPR allocation.

4 Conclusion and discussion

This paper develops a meso-scale system representation model to approximate large water systems with reduced backbone networks. The meso-scale representation has reduced model complexity, retains key physical behaviors, and enables computational policy search for DWSs. The meso-scale modeling approach is extendable to more general integrated water systems to understand the complex interaction dynamics between subsystems and global systems.

We also formulate a multi-objective optimization model on reduced backbone networks to search for optimal DWSs with distributed DPR. We consider two performance objectives, economic cost, and energy consumption relevant to infrastructure investment, water treatment, and water distribution. We also manage two configuration decision variables, locations, and treatment scales of DPR facilities, under constraints of local and global demand satisfaction, predetermined available sites and capacities of DPR plants, and hydraulic and operational requirements.

We demonstrate our methods on a hypothetical DWS from the real water and wastewater infrastructure data of the City of Houston. Our meso-scale representation reduces 95% of edges and 93% of nodes, while achieving good approximations of macro-scale flows with relative difference of outflows from the three centralized WWTPs–of up to 1.44%. It makes optimization analysis computationally feasible by reducing the complexity of the system model. Also, we get satisfactory approximation of meso-scale node pressures with relative difference in 81% of nodes being within $[-10\%,\ 10\%]$. In addition to these basic system responses, the meso-scale backbone network model allows estimation of performance measures that are not tractable with the full water network model, including the spatial distribution of water demands and energy intensities. These meso-scale performance measures lay the foundation for computational policy search of DWSs.

The multi-objective optimization analysis of the Houston DWS reveals context-specific as well as general opportunities, constraints, and their interactions for allocating distributed DPR. Location is the most critical factor for implementing DPR because of the large variation of energy intensities within the Houston DWS. In part of the western areas, high energy intensities are due to long conveyance distance from the centralized WTPs, while in other areas, high energy consumption comes from energy-intensive groundwater supply. In such areas, if there are considerable water demands, and the available wastewater reuse capacities can match the magnitudes of the water demands, implementing distributed DPR can achieve system-wide benefits. Moreover, there are trade-offs between energy consumption and economic cost with different DPR allocation

configurations.

In addition to energy consumption and economic cost, there are other important criteria driving the design and implementation of DWSs such as water supply resiliency, water resource sustainability, and water quality. As conventional water systems rely on surface water and groundwater supply, they are becoming more vulnerable to climate change impacts that threaten water supply reliability, water availability, and surface water quality (van de Lindt et al., 2020; Alam et al., 2021; Khan et al., 2015; Tampa Bay Water, 2018; Nielsen-Gammon, 2012). Further research on policy search of DWSs considering these multiple criteria is needed to facilitate implementation of DWSs.

The DWSs considered in this study are simplified. We constrained the locations of DPR plants to the existing sites of WWTPs and we do not model individual distributed subsystems. In practice, there can be advanced treatment trains constructed as separate facilities (Sim & Mauter, 2021), and new WWTPs with advanced treatment. Fortunately, meso-scale modeling of the fully integrated water and wastewater system still facilitates policy search across a much larger design space. Also, directly connecting a DPR plant with the existing centralized systems is a desirable first step towards DWS. Here, collective functionality assures redundancy, while independence maintains modularity. We need more comprehensive complex network analyses (e.g., Romero, 2021) to guide the topology design for DWSs that are robust under both normal and contingency conditions.

Acknowledgments

The authors acknowledge funding from the National Science Foundation (award no. CBET-1707117). We appreciate data support from M. Ramon, P. Pradhan and F. Rabbi from Houston Public Works.

Open Research

The software WNTR used for hydraulic modeling is an open-source Python package available from its website https://wntr.readthedocs.io/en/latest/installation.html. The Python package Pymoo we use for Non-dominated Sorting Genetic Algorithm-II implementation is also publicly available from its website https://pymoo.org/installation.html. The code for meso-scale modeling and multiple objective optimization is available at this Github repository https://github.com/Zhouxiaomu33/Code-for-mesoscale-modeling-and-multiobjective-optimization-.

References

Alam, S., Gebremichael, M., Ban, Z., Scanlon, B. R., Senay, G., & Lettenmaier, D. P. (2021). Post-drought groundwater storage recovery in California's Central Valley. *Water Resources Research*, *57*(10). https://doi.org/10.1029/2021wr030352

ASCE. (2021). *Failure to Act: Economic Impacts of Status Quo Investment*

Across Infrastructure Systems.

AWWA. (2011). *Buried no longer challenge: confronting America's water infrastructure*. Technical report, American Water Works Association, Denver, CO, USA.

Biggs, C., Ryan, C., Wiseman, J., and Larsen, K. (2009). *Distributed water systems: A networked and localized approach for sustainable water services*. Technical report, VEIL.

Blank, J., & Deb, K. (2020). Pymoo: Multi-Objective Optimization in Python. *IEEE Access: Practical Innovations, Open Solutions*, *8*, 89497–89509. https://doi.org/10.1109/access.2020.2990567

Crosson, C., Achilli, A., Zuniga-Teran, A. A., Mack, E. A., Albrecht, T., Shrestha, P., Boccelli, D. L., Cath, T. Y., Daigger, G. T., Duan, J., Lansey, K. E., Meixner, T., Pincetl, S., & Scott, C. A. (2021). Net zero urban water from concept to applications: Integrating natural, built, and social systems for responsive and adaptive solutions. *ACS ES&T Water*, *1*(3), 518–529. https://doi.org/10.1021/acsestwater.0c00180

Dai, L., Derudder, B., & Liu, X. (2018). Transport network backbone extraction: A comparison of techniques. *Journal of Transport Geography*, *69*, 271–281. https://doi.org/10.1016/j.jtrangeo.2018.05.012

Darabos, C., White, M. J., Graham, B. E., Leung, D. N., Williams, S. M., & Moore, J. H. (2014). The multiscale backbone of the human phenotype network based on biological pathways. *BioData Mining*, *7*(1), 1. https://doi.org/10.1186/1756-0381-7-1

Deb, K., Pratap, A., Agarwal, S., & Meyarivan, T. (2002). A fast and elitist multiobjective genetic algorithm: NSGA-II. *IEEE Transactions on Evolutionary Computation : A Publication of the IEEE Neural Networks Council*, *6*(2), 182–197. https://doi.org/10.1109/4235.996017

Diao, K. (2021). Towards resilient water supply in centralized control and decentralized execution mode. *Journal of Water Supply Research and Technology—AQUA*, *70*(4), 449–466. https://doi.org/10.2166/aqua.2021.162

Diffenbaugh, N. S., Swain, D. L., & Touma, D. (2015). Anthropogenic warming has increased drought risk in California. *Proceedings of the National Academy of Sciences of the United States of America*, *112*(13), 3931–3936. https://doi.org/10.1073/pnas.1422385112

Ducruet, C. (2017). Multilayer dynamics of complex spatial networks: The case of global maritime flows (1977–2008). *Journal of Transport Geography*, *60*, 47–58. https://doi.org/10.1016/j.jtrangeo.2017.02.007

Englehardt, J. D., Wu, T., Bloetscher, F., Deng, Y., du Pisani, P., Eilert, S., Elmir, S., Guo, T., Jacangelo, J., LeChevallier, M., Leverenz, H., Mancha, E., Plater-Zyberk, E., Sheikh, B., Steinle-Darling, E., & Tchobanoglous, G. (2016).

Net-zero water management: achieving energy-positive municipal water supply. *Environmental Science: Water Research & Technology*, *2*(2), 250–260. https://doi.org/10.1016/j.jtrangeo.2017.02.007

EPA, U. S. (2020). EPANET. Retrieved from https://www.epa.gov/water-research/epanet

Ferrario, E., Pedroni, N., & Zio, E. (2016). Evaluation of the robustness of critical infrastructures by Hierarchical Graph representation, clustering and Monte Carlo simulation. *Reliability Engineering & System Safety*, *155*, 78–96. https://doi.org/10.1016/j.ress.2016.06.007

Flörke, M., Schneider, C., & McDonald, R. I. (2018). Water competition between cities and agriculture driven by climate change and urban growth. *Nature Sustainability*, *1*(1), 51–58. https://doi.org/10.1038/s41893-017-0006-8

Foti, N. J., Hughes, J. M., & Rockmore, D. N. (2011). Nonparametric sparsification of complex multiscale networks. *PloS One*, *6*(2), e16431. https://doi.org/10.1371/journal.pone.0016431

Gemmetto, V., Cardillo, A., & Garlaschelli, D. (2017). Irreducible network backbones: unbiased graph filtering via maximum entropy. In *arXiv* [*physics.soc-ph*]. http://arxiv.org/abs/1706.00230

Gómez, C., Sanchez-Silva, M., Dueñas-Osorio, L., & Rosowsky, D. (2013). Hierarchical infrastructure network representation methods for risk-based decision-making. *Structure and Infrastructure Engineering: Maintenance, Management, Life-Cycle Design and Performance*, *9*(3), 260–274. https://doi.org/10.1080/15732479.2010.546415

Gray, E., NASA's Earth Science News Team, Merzdorf, J., & NASA's Goddard Space Flight Center. (2019, June 13). Earth's freshwater future: Extremes of flood and drought. Retrieved June 1, 2021, from Climate Change: Vital Signs of the Planet website: https://climate.nasa.gov/news/2881/earths-freshwater-future-extremes-of-flood-and-drought/

He, C., Liu, Z., Wu, J., Pan, X., Fang, Z., Li, J., & Bryan, B. A. (2021). Future global urban water scarcity and potential solutions. *Nature Communications*, *12*(1), 4667. https://doi.org/10.1038/s41467-021-25026-3

Hébert-Dufresne, L., Grochow, J. A., & Allard, A. (2016). Multi-scale structure and topological anomaly detection via a new network statistic: The onion decomposition. *Scientific Reports*, *6*(1). https://doi.org/10.1038/srep31708

Hering, J. G., Waite, T. D., Luthy, R. G., Drewes, J. E., & Sedlak, D. L. (2013). A changing framework for urban water systems. *Environmental Science & Technology*, *47*(19), 10721–10726. https://doi.org/10.1021/es4007096

Herrera-García, G., Ezquerro, P., Tomás, R., Béjar-Pizarro, M., López-Vinielles, J., Rossi, M., Mateos, R. M., Carreón-Freyre, D., Lambert, J., Teatini, P., Cabral-Cano, E., Erkens, G., Galloway, D., Hung, W.-C., Kakar, N., Sneed,

M., Tosi, L., Wang, H., & Ye, S. (2021). Mapping the global threat of land subsidence. *Science (New York, N.Y.)*, *371*(6524), 34–36. https://doi.org/10.1126/science.abb8549

Hoffmann, S., Feldmann, U., Bach, P. M., Binz, C., Farrelly, M., Frantzeskaki, N., Hiessl, H., Inauen, J., Larsen, T. A., Lienert, J., Londong, J., Lüthi, C., Maurer, M., Mitchell, C., Morgenroth, E., Nelson, K. L., Scholten, L., Truffer, B., & Udert, K. M. (2020). A research agenda for the future of urban water management: Exploring the potential of nongrid, small-grid, and hybrid solutions. *Environmental Science & Technology*, *54*(9), 5312–5322. https://doi.org/10.1021/acs.est.9b05222

Houston Public Works (a). Drinking Water Operations. Retrieved July 8, 2021, from Houstontx.gov website: https://www.publicworks.houstontx.gov/pud/drinkingwater.html

Houston Public Works (b). Daily Water Supply Monitor. Retrieved July 12, 2021, from https://www.publicworks.houstontx.gov/pud/dwsm.html

Houston Public Works. (2019). Water conservation plan.

Harris Galveston Subsidence District. (2019, September 16). Retrieved September 29, 2021, from Hgsubsidence.org website: https://hgsubsidence.org/

Jasechko, S., Perrone, D., Seybold, H., Fan, Y., & Kirchner, J. W. (2020). Groundwater level observations in 250,000 coastal US wells reveal scope of potential seawater intrusion. *Nature Communications*, *11*(1), 3229. https://doi.org/10.1038/s41467-020-17038-2

Jensen, O., & Khalis, A. (2020). Urban water systems: Development of micro-level indicators to support integrated policy. *PloS One*, *15*(2), e0228295. https://doi.org/10.1371/journal.pone.0228295

Jones, E. C., & Leibowicz, B. D. (2021). Co-optimization and community: Maximizing the benefits of distributed electricity and water technologies. Sustainable Cities and Society, 64(102515), 102515. https://doi.org/10.1016/j.scs.2020.102515

Kavvada, O., Nelson, K. L., & Horvath, A. (2018). Spatial optimization for decentralized non-potable water reuse. *Environmental Research Letters*, *13*(6), 064001. https://doi.org/10.1088/1748-9326/aabef0

Khan, S. J., Deere, D., Leusch, F. D. L., Humpage, A., Jenkins, M., & Cunliffe, D. (2015). Extreme weather events: Should drinking water quality management systems adapt to changing risk profiles? *Water Research*, *85*, 124–136. https://doi.org/10.1016/j.watres.2015.08.018

Klise, K. A., Bynum, M., Moriarty, D., & Murray, R. (2017). A software framework for assessing the resilience of drinking water systems to disasters with an example earthquake case study. *Environmental Modelling & Software: With*

Environment Data News, *95*, 420–431. https://doi.org/10.1016/j.envsoft.2017.06.022

Larsen, T. A., Hoffmann, S., Lüthi, C., Truffer, B., & Maurer, M. (2016). Emerging solutions to the water challenges of an urbanizing world. *Science (New York, N.Y.)*, *352*(6288), 928–933. https://doi.org/10.1126/science.aad8641

Leigh, N., & Lee, H. (2019). Sustainable and resilient urban water systems: The role of decentralization and planning. *Sustainability*, *11*(3), 918. https://doi.org/10.3390/su11030918

Liu, L., Lopez, E., Dueñas-Osorio, L., Stadler, L., Xie, Y., Alvarez, P. J. J., & Li, Q. (2020). The importance of system configuration for distributed direct potable water reuse. Nature Sustainability, 3(7), 548–555. https://doi.org/10.1038/s41893-020-0518-5

Liu, Y., & Mauter, M. S. (2021). Marginal energy intensity of water supply. *Energy & Environmental Science*, *14*(8), 4533–4540. https://doi.org/10.1039/d1ee00925g

Makropoulos, C. K., & Butler, D. (2010). Distributed water infrastructure for sustainable communities. *Water Resources Management*, *24*(11), 2795–2816. https://doi.org/10.1007/s11269-010-9580-5

Mones, E., Vicsek, L., & Vicsek, T. (2012). Hierarchy measure for complex networks. *PloS One*, *7*(3), e33799. https://doi.org/10.1371/journal.pone.0033799

National Research Council, 2011. Water Reuse: Potential for Expanding the Nation's Water Supply through Reuse of Municipal Wastewater. The National Academies Press, Washington, DC, USA.

Neal, Z. (2014). The backbone of bipartite projections: Inferring relationships from co-authorship, co-sponsorship, co-attendance and other co-behaviors. *Social Networks*, *39*, 84–97. https://doi.org/10.1016/j.socnet.2014.06.001

Nielsen-Gammon, J. W. (2012). The 2011 Texas drought. *Texas Water Journal*, 3(1), 59-95.

Porse, E., Mika, K. B., Litvak, E., Manago, K. F., Hogue, T. S., Gold, M., Pataki, D. E., & Pincetl, S. (2018). The economic value of local water supplies in Los Angeles. *Nature Sustainability*, *1*(6), 289–297. https://doi.org/10.1038/s41893-018-0068-2

Pumain, D. (Ed.). (2005). *Hierarchy in Natural and Social Sciences* (2006th ed.). New York, NY: Springer.

Romero, P. (2021). Uniformly optimally reliable graphs: A survey. Networks (New York, NY). https://doi.org/10.1002/net.22085

Scott Vitter, J., Jr, Berhanu, B., Deetjen, T. A., Leibowicz, B. D., & Webber, M. E. (2018). Optimal sizing and dispatch for a community-scale potable water

recycling facility. *Sustainable Cities and Society*, *39*, 225–240. https://doi.org/10.1016/j.scs.2018.02.023

Sharma, A., Burn, S., Gardner, T., & Gregory, A. (2010). Role of decentralised systems in the transition of urban water systems. *Water Science & Technology: Water Supply*, *10*(4), 577–583. https://doi.org/10.2166/ws.2010.187

Sim, A., & Mauter, M. S. (2021). Cost and energy intensity of U.S. potable water reuse systems. *Environmental Science: Water Research & Technology*, *7*(4), 748–761. https://doi.org/10.1039/d1ew00017a

Tampa Bay Water. (2018). Long-term Master Water Plan.

Twomey, K. M., & Webber, M. E. (2011). Evaluating the energy intensity of the US public water system. *ASME 2011 5th International Conference on Energy Sustainability, Parts A, B, and C*. ASMEDC.

van de Lindt, J. W., Peacock, W. G., Mitrani-Reiser, J., Rosenheim, N., Deniz, D., Dillard, M., Tomiczek, T., Koliou, M., Graettinger, A., Crawford, P. S., Harrison, K., Barbosa, A., Tobin, J., Helgeson, J., Peek, L., Memari, M., Sutley, E. J., Hamideh, S., Gu, D., … Fung, J. (2020). Community resilience-focused technical investigation of the 2016 Lumberton, North Carolina, flood: An interdisciplinary approach. *Natural Hazards Review*, *21*(3), 04020029. https://doi.org/10.1061/(asce)nh.1527-6996.0000387

Walski, T.M., Chase, D.V., Savic, D.A., Grayman, W., Beckwith, S. *Advanced water distribution modeling and management*. (2003). Haestead Press, Waterbury, CT, 693p.

Zhang, Q. H., Yang, W. N., Ngo, H. H., Guo, W. S., Jin, P. K., Dzakpasu, M., Yang, S. J., Wang, Q., Wang, X. C., & Ao, D. (2016). Current status of urban wastewater treatment plants in China. *Environment International*, *92–93*, 11–22. https://doi.org/10.1016/j.envint.2016.03.024

Zodrow, K. R., Li, Q., Buono, R. M., Chen, W., Daigger, G., Dueñas-Osorio, L., Elimelech, M., Huang, X., Jiang, G., Kim, J.-H., Logan, B. E., Sedlak, D. L., Westerhoff, P., & Alvarez, P. J. J. (2017). Advanced materials, technologies, and complex systems analyses: Emerging opportunities to enhance urban water security. *Environmental Science & Technology*, *51*(18), 10274–10281. https://doi.org/10.1021/acs.est.7b01679

References From the Supporting Information

Emmerich, M. T. M., & Deutz, A. H. (2018). A tutorial on multiobjective optimization: fundamentals and evolutionary methods. *Natural Computing*, *17*(3), 585–609. https://doi.org/10.1007/s11047-018-9685-y

Bertazzi, L., & Wang, X. (2022). Matheuristics with performance guarantee for the unsplit and split delivery capacitated vehicle routing problem. *Networks (New York, NY)*. https://doi.org/10.1002/net.22115